Journal of Computational Physics 249 (2013) 13–21

Contents lists available at SciVerse ScienceDirect

Journal of Computational Physics

journal homepage: www.elsevier.com/locate/jcp

A Monte Carlo algorithm for degenerate plasmas

A.E. Turrell *, M. Sherlock, S.J. Rose

Blackett Laboratory, Imperial College London, South Kensington SW7 2AZ, United Kingdom

ARTICLE INFO

Article history:
Received 29 October 2012
Received in revised form 26 March 2013
Accepted 30 March 2013
Available online 10 April 2013

Keywords:
Monte Carlo
Degenerate plasma

ABSTRACT

A procedure for performing Monte Carlo calculations of plasmas with an arbitrary level of degeneracy is outlined. It has possible applications in inertial confinement fusion and astrophysics. Degenerate particles are initialised according to the Fermi–Dirac distribution function, and scattering is via a Pauli blocked binary collision approximation. The algorithm is tested against degenerate electron–ion equilibration, and the degenerate resistivity transport coefficient from unmagnetised first order transport theory. The code is applied to the cold fuel shell and alpha particle equilibration problem of inertial confinement fusion.

1. Introduction

The degenerate Monte Carlo algorithm is based on the binary collision approximation Monte Carlo code of Takizuka and Abe [1], which randomly pairs particles in close proximity and scatters them with Coulomb collisions, each one of which conserves energy and momentum. Apart from conservation, the greatest strength of this approach is the ability to work with any distribution function, especially those which depart appreciably from a Maxwell–Boltzmann distribution - it has been used, for instance, to reproduce and study the Langdon distribution [2,3]. It has been extended several times [4,5], and we offer an extension to degenerate plasmas.

Modelling degenerate plasmas is of interest in inertial confinement fusion, during compression of the cold fuel and capsule shell [6,7], and in astrophysical situations such as white dwarf stars [8]. Relevant inertial confinement fusion problems are degenerate thermal equilibration and the stopping of high energy ions by degenerate electrons. The yield is particularly sensitive to electron–ion equilibration, with simulations of direct-drive implosions showing a $\sim$10% difference across several different models of temperature relaxation [9]. Examples of equilibration are presented for a range of degeneracies. There are potential applications in transport theory, and we show that the degenerate resistivity transport coefficient is reproduced for 1st order unmagnetised transport theory.

The algorithm allows the modelling of plasmas of arbitrary degeneracy under the binary collision approximation. It uses a numerical interpolation of the inverse cumulative density function of the Fermi–Dirac distribution to initialise simulation particles, and collisions are subject to Pauli blocking. It is not appropriate in the limit of very strong coupling because the plasma theory which the Monte Carlo code is based on breaks down. The strong coupling limit corresponds to $\ln\Lambda \lesssim 3$, with $\ln\Lambda$ the Coulomb logarithm [10]. The code is designed for $\ln\Lambda > 3$ in collisional plasmas with a non-negligible level of degeneracy. It is noted that Monte Carlo techniques with degenerate capabilities have been developed for studying transport in semi-conductors [11] but no such method exists for fully-ionised plasmas. Some of the techniques described are potentially applicable to other types of codes, for example, Particle-In-Cell (PIC) codes.

* Corresponding author. Tel.: +442075943791.
E-mail address: a.turrell09@imperial.ac.uk (A.E. Turrell).

0021-9991
http://dx.doi.org/10.1016/j.jcp.2013.03.052

2. Degenerate plasmas

This discussion is with respect to degenerate electrons but the process is the same for any fermion. Applying the anti-commutation relation for identical fermions to free electrons gives rise to the Fermi–Dirac distribution [12];

$$f(E)dE = \frac{(2m_e)^{3/2}}{2n_e\hbar^3\pi^2}\frac{\sqrt{E}dE}{\exp\{\frac{E}{T_e}-\eta\}+1}$$

where η is the degeneracy parameter. $f(E)dE$ is normalised to 1, and the equation

$$\int \frac{(2m_e)^{3/2}}{2n_e\hbar^3\pi^2}\frac{\sqrt{E}dE}{\exp\{\frac{E}{T_e}-\eta\}+1} = 1 \tag{1}$$

defines η as a function of n_e and T_e. The occupancy function is the measure of the proportion of states occupied at energy E, and is given by

$$f_o(E) = \frac{1}{\exp\{\frac{E}{T_e}-\eta\}+1} = f(E)/g(E) \tag{2}$$

where $g(E)dE = \frac{(2m_e)^{3/2}}{2n_e\hbar^3\pi^2}\sqrt{E}dE$ is the density of states between E and $E+dE$. $\eta \longrightarrow -\infty$ corresponds to the classical limit in which the distribution function becomes a Maxwell–Boltzmann distribution. $\eta \longrightarrow \infty$ is the fully degenerate limit in which the all of the particles are at energies below or equal to the Fermi energy, E_F, and the occupancy function becomes a step function

$$g(E) = 1, \quad E \leqslant E_F; \quad g(E) = 0, \quad E > E_F$$

where

$$E_F = \frac{\hbar^2}{2m_e}\left(3\pi^2 n_e\right)^{2/3}$$

is the Fermi energy. For a non-Maxwellian distribution, temperature and average energy no longer satisfy $T_e = \frac{2}{3}\langle E\rangle$. In the case of the Fermi–Dirac distribution, particles retain an energy even in the $T_e \longrightarrow 0$ limit as lower energy states have limited capacity and become fully occupied, so that remaining particles occupy energy states higher than the ground state. In the zero temperature limit,

$$\eta \longrightarrow \frac{E_F}{T_e} \text{ and } \eta \longrightarrow \infty \tag{3}$$

There are many choices for the Coulomb logarithm for electron–ion equilibration in a degenerate plasma [13,14,10]. The code does not explicitly require a particular Coulomb logarithm, and any could be used in the algorithm, as long as they include degeneracy effects. Degenerate modifications are necessary, because of the disparity between temperature and average energy, and the potential for degenerate plasmas to occur at high density. We use Gericke, Murrillo and Schlanges' Coulomb logarithm number 6 [10] but, due to the possibility of encountering the $T_e \longrightarrow 0$ limit, we replace T_e by the 'effective' temperature defined by $T'_e = \sqrt{T_F^2 + T_e^2}$ where T_F is the Fermi temperature. This is the same approximation as used by several other authors including Brown and Haines [15], and Brysk, Campbell and Hammerling [16] who demonstrated that it matches Salpeter's [17] relation, where the $T_e \longrightarrow 0$ limit is avoided by multiplying by a factor $I_{1/2}(\eta)/I'_{1/2}(\eta)$, to within 5% for any η. $I_j(\eta)$ is the jth complete Fermi–Dirac integral. This gives,

$$\ln\Lambda_{ie} = \frac{1}{2}\ln\left[1 + \frac{b_{\mathrm{M}}^2}{b_{\mathrm{m},ie}^2}\right]$$

for an electron and i an ion, with 'M' denoting 'maximum', and 'm' 'minimum' in the impact parameters. The maximum is given by

$$b_{\mathrm{M}}^2 = \lambda_D^2 + r_{\mathrm{ion}}^2$$

where $r_{\mathrm{ion}} = \left(4\pi\sum_{\mathrm{ions}} n_i/3\right)^{-1/3}$ is the inter-ion distance [17] and λ_D is the Debye length, while the minimum is given by

$$b_{\mathrm{m},ie}^2 = \lambda_{dB}^2 + b_{\perp}^2$$

where

$$\lambda_{dB} = \frac{\hbar}{2}\frac{1}{\sqrt{m_e T'_e}}$$

is the de Broglie wavelength of the electrons, and represents their closest distance of approach to ions in the quantum mechanical limit, and

$$b_\perp = \frac{eq_i}{4\pi\epsilon_0}\frac{1}{T_e'}$$

is the classical closest distance of approach for electron–ion centre-of-mass scattering through $\pi/2$ with q_i the charge of ion species i.

3. Description of the method

The Monte Carlo code is adapted to include Pauli blocking and the ability to initialise species with Fermi–Dirac distributions if required, as well as generating Maxwell–Boltzmann distributions. Maxwellian distributions are initialised using the computationally efficient Box-Muller transform [18]. For distributions which are everywhere integrable, the probability density function (or distribution function) can be integrated to the cumulative density function $\int_0^x f(x')dx' = F(x)$ and the cumulative density function normalised such that $F(0) = 0$ and $\lim_{x\to\infty} F(x) = 1$. The cumulative density function is inverted:

$$F^{-1}(u) = x; \quad u \in (0,1)$$

This represents a parametrisation of the real number line between 0 and 1 into the space of the variable. Randomly generated values of u, uniformly distributed and in the domain of $F^{-1}(u)$, generate values of x that occur with frequencies determined by the original probability density function.

The Fermi–Dirac distribution is not integrable so this process cannot be done analytically, and numerical methods of calculating the inverse cumulative distribution function must be used. Numerical computations of energy values for initialising particles employ Hörmann and Leydold's algorithm [19]. It requires evaluations of $f(E), F(E)$ and initial boundary conditions. The domain of $F^{-1}(u)$ is split into equally spaced sub-intervals and a cubic Hermite polynomial $H_i(u)$ is used to interpolate values of E given u, with $F(E)_i \leqslant u \leqslant F(E)_{i+1}$. Cubic Hermite polynomials have advantages over other methods of interpolation of the same order because they are a local approximation, rather than a global one: if any interval does not reach the required level of approximation to the inverse cumulative distribution function, new points can be inserted locally without recomputing all interpolation points. Another advantage is that there is a relatively simple algorithm, which terminates if $f(E)$ is continuous, that can guarantee the monotonicity of $H_i(u)\,\forall\, i$ by creating new interpolation points [20]. Linear interpolation is also guaranteed to be monotonically increasing, but the number of points required for the same level of approximation to $F^{-1}(u)$ is generally reduced by an order of magnitude or more by using cubic interpolation [19]. For the entire interpolation process, the maximal acceptable error

$$\epsilon_u = \max_{u\in[u_i,u_{i+1}]} |F(H_i(u)) - u|$$

can be specified, and intervals are split until this is satisfied for every i. The end result is a table of values of $[u_i = F(x_i), x_i, f(x_i)]$.

With the creation of the table, values of u can be generated and the appropriately distributed values of E found. An indexed search is used to speed up the process of selecting an appropriate E for the given value of u [21]. Components of velocity must also be selected. For an isotropic distribution of velocities, each energy can be thought of as defining a value of the radius of a sphere in velocity space, and randomly choosing a point on a 2-sphere, then scaling the values by $v = \sqrt{2E/m_e}$, gives the components of each particle's velocity:

$$v_x = v\sqrt{1-r^2}\cos\phi$$

$$v_y = v\sqrt{1-r^2}\sin\phi$$

$$v_z = vr$$

where $r \in [-1,1]$ and $\phi \in [0, 2\pi)$.

Initialised Fermi–Dirac distributions relax to Maxwell–Boltzmann distributions without Pauli blocking. To prevent this, all processes which lead to a change in a simulation particle's energy, such as scattering or acceleration by an electric field, must be subject to Pauli blocking. The blocking process must prevent electrons being scattering into an energy state E if that state is already occupied. The occupancy function, Eq. (2), is the measure of the proportion of states occupied at energy E. $f_o(E)$ takes values between 0 and 1 and, from the point of view of Monte Carlo simulation, indicates whether a particular energy changing process should be blocked or not. The probability of accepting a change in electron energy to final energy E' should be $P = 1 - f_o(E')$ so that fully occupied states admit no more particles. This is consistent with the $(1 - f_0(E'))$ factor in the effective cross-section in Eq. (15) of Brysk's derivation of degenerate stopping and equilibration rates [22], and also in Eq. (7.1) of Brown and Singleton's Boltzmann collision operator with Fermi–Dirac statistics [14], which relaxes distributions to Fermi–Dirac distribution functions. The probability of accepting a new energy state is dependent on the degeneracy, so that the classical limit of $\eta \to -\infty, f_o(E') \to 0\,\forall E'$ is reproduced. Fig. 1 shows a Fermi–Dirac distribution generated by the code at the start of a simulation, and its associated occupancy function.

To perform the Pauli blocking on changes in particle energy such that the final energy is E', the Monte Carlo simulation generates a random number R and uses the following procedure

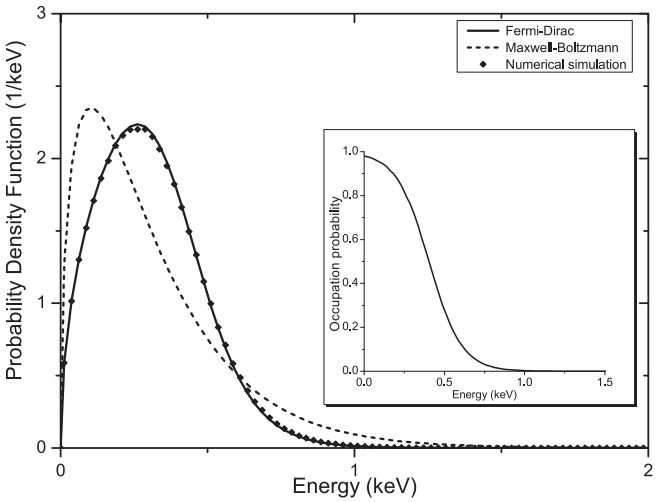

Fig. 1. The degenerate Monte Carlo algorithm producing a 0D3V Fermi–Dirac distribution of electrons, for $T_e = 100$ eV, $n_e = 8 \times 10^{31}\mathrm{m}^{-3}$ and $\eta = 4.2$. It is shown against Maxwell–Boltzmann and Fermi–Dirac distributions with the same parameters. There is good agreement between the analytic, and numerically generated, Fermi–Dirac distributions. INSET: The occupation function sampled from the simulation distribution function.

$$\text{For } R \in (0,1) \text{ and } E' \begin{cases} \text{Block the change} & \text{if } R < f_o(E'); \\ \text{accept the change} & \text{if } R > f_o(E'). \end{cases} \tag{4}$$

For two-body processes, such as fermion-fermion scattering, this has a natural extension; with final energies E'_1 and E'_2, if,

$$R < f_o(E'_1) + f_o(E'_2) - f_o(E'_1) f_o(E'_2)$$

is true then the process is Pauli blocked. $f_o(E') = 0 \forall E'$ for non-degenerate particles.

Simulations on an initial Fermi–Dirac distribution, Fig. 2, show that including the Pauli blocking algorithm maintains the distribution function, Fig. 3.

The average electron energy is recorded from the Monte Carlo simulation. However, diagnosing the electron temperature and degeneracy parameter from the average energy is non-trivial. The method employed is to calculate the probability density function from simulation, $f_{\mathrm{MC}}(E_i)dE$, in a number of bins. Then T_e, and therefore η by Eq. (1), can be varied until the root sum of square differences between the simulation distribution and the Fermi–Dirac distribution is minimised. The root sum of squares is

$$\sqrt{\sum_i \left(f_{\mathrm{MC}}(E_i)dE - f(E_i, T_e, \eta)dE\right)^2}$$

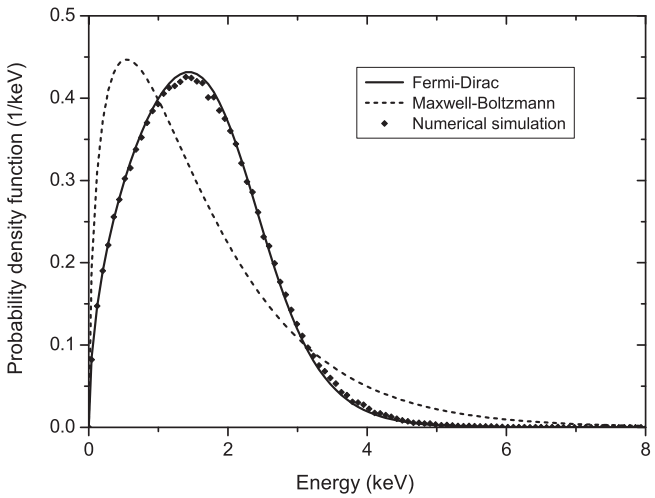

Fig. 2. An electron distribution generated by the code and initialised with $n_e = 10^{33}\mathrm{m}^{-3}, T_e = 0.47$ keV and $\eta = 4.7$. It is shown against the analytical Maxwell–Boltzmann and Fermi–Dirac distributions with the same parameters.

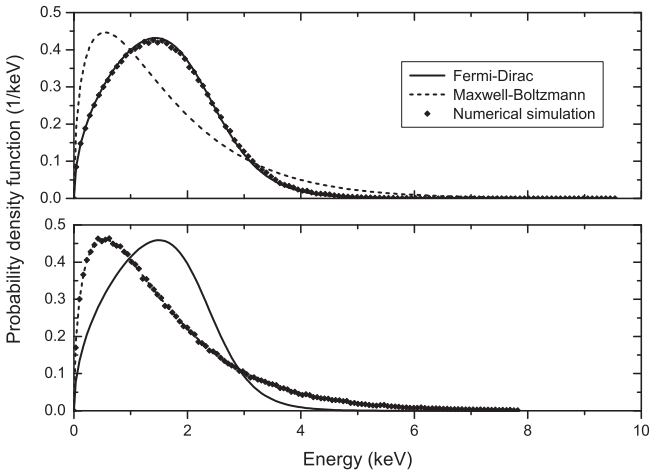

Fig. 3. The distributions from Fig. 2 after 0.16 fs. The numerical simulation with Pauli blocking (top) matches the analytical Fermi–Dirac distribution with the same parameters, but the run with the Pauli blocking disabled (bottom) has relaxed to a Maxwell–Boltzmann distribution.

A golden section search [23] is used for the minimisation of the root sum square, and calculation of T_e. Initial guesses of $T^* \approx T_e$ and bounding values T_{Max} and T_{Min} are required for the golden section search, where $T_{\text{Min}} < T^* < T_{\text{Max}}$. As

$$\langle E \rangle = \frac{3\sqrt{\pi}}{8} \frac{T_e}{n_e} \frac{(2m_e T_e)^{3/2}}{\hbar^3 \pi^2} I_{3/2}(\eta) \tag{5}$$

where $\lim_{\eta \to -\infty} \langle E \rangle = \frac{3}{2} T_e$, and $\lim_{\eta \to \infty} \langle E \rangle = \frac{3}{5} E_F$,

$$T^* = \sqrt{(2\langle E \rangle/3)^2 - (2E_f/5)^2}$$

is used as the initial guess, with T_{Max} and T_{Min} given, for example, by $T^* \pm 10\%$ respectively.

4. Tests

The rate of electron–ion temperature equilibration is given by

$$\frac{dT_i}{dt} = \sum_i \nu_{ie}(T_e - T_i) \tag{6}$$

where i denotes an ion species. Spitzer's equilibration rate [24] fails for weakly to strongly degenerate plasmas. Brysk [22] derived an equilibration formula appropriate for degenerate conditions in which $T_i/m_i \ll T_e/m_e$;

$$\nu_{ie} = \frac{8}{3} \left(\frac{q_i e}{4\pi\epsilon_0} \right)^2 \frac{m_e^2 \ln \Lambda_{ie}}{\pi m_i \hbar^3 (1 + e^{-\eta})} \tag{7}$$

Fig. 4 compares the non-degenerate rate, the degenerate rate, and the degenerate Monte Carlo algorithm for a range of degeneracies, with varying initial temperatures and densities.

The numerical equilibration rate to non-degenerate equilibration rate ratio for $\eta = 8.1$ is omitted as the non-degenerate electron temperature never reached 90% of the final temperature. This is because it is implicitly assumed that $T_e = \frac{2}{3}\langle E \rangle_e$ in the non-degenerate rate. The total energy in the degenerate case is higher though, as degenerate particles retain an energy even in the $T_e \to 0$ limit. In scenarios where η drops over time, Eq. (5) forces T_e to rise for fixed $\langle E \rangle_e$. In a situation with $T_{i,0} > T_{e,0}$, this means that the classical $T_{e,f}$ may never reach the same, or a fraction of the same, value as in the degenerate case. An extreme case illustrates this more clearly; initial temperatures of two species, ions and electrons, with $T_{i,0} \gg T_{e,0}$ give a classical end temperature of $T_f = (T_{i,0} + T_{e,0})/2 \approx T_{i,0}/2$ for both electrons and ions. But if $T_{e,0} \ll T_F \ll T_{i,0}$, where T_F is the Fermi temperature, and the ions provide enough energy to force the electron distribution to become Maxwellian, the end temperature will be $T_f \approx (T_{i,0} + T_F)/2 > T_{i,0}/2$. The $\eta = 8.1$ data point has a lower $T_{i,0}/T_{e,0}$ ratio than that at the highest η plotted, but $T_F/T_{i,0}$ is higher so the disparity in final temperatures between the classical and degenerate cases is expected.

The agreement between the degenerate equilibration rate and the degenerate Monte Carlo equilibration rate is good for a range of initial values of the degeneracy, but does show variation. The origin of this variability is the inherent noisiness of Monte Carlo simulations (as only a finite number of particles can be simulated), but in general the models agree, and the

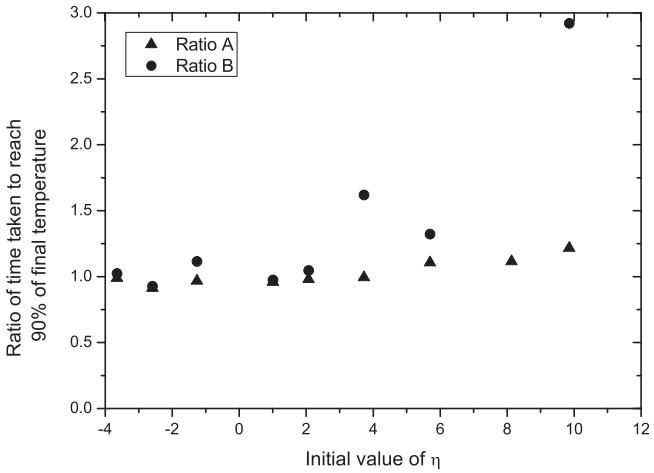

Fig. 4. Equilibration with a range of starting electron and deuterium temperatures and densities, classified by initial electron degeneracy, η. The ratios shown are of the time taken to reach 90% of the final temperature as given by numerical simulation. Ratio A is of the degenerate Monte Carlo equilibration rate to the degenerate equilibration rate. Ratio B is of the degenerate numerical equilibration rate to the non-degenerate equilibration rate. The numerical equilibration rate to non-degenerate equilibration rate ratio for $\eta = 8.1$ is omitted as the non-degenerate electron temperature never reached 90% of the final temperature.

mean ratio across all of the equilibrations is 1.03. There is a slight upward trend in Ratio A, that is the ratio of the time taken to reach 90% of the final temperature of the Monte Carlo algorithm relative to theory as governed by Eq. (6). This slight trend is probably partly due to small errors in diagnosing T_e from the Monte Carlo simulation, and partly due to evaluation of (6). In the degenerate theory, computation of new values of T_e and η using $\frac{d\langle E\rangle_e}{dt}$ from (6) self-consistently is non-trivial, and there are leading order corrections to (7) which are of relative size $\sim T_i m_e/T_e m_i$. All of these are sources of error which are worse at high degeneracy, but which affect the time taken to reach equilibration only slightly for regimes of physical interest.

As a further verification of the algorithm, we reproduce degenerate resistivities from un-magnetised transport theory, assuming isotropic temperature and pressure. Restricting the current density to the x direction, the resistivity of the plasma is given by $\rho = E_x/J_x$. First order transport theory [25,26] gives the resistivity without electron–electron collisions (known as the Lorentz limit), as

$$\rho = 3m_e n_i \frac{\ln\Lambda_{ie}}{e^2}\left(\frac{-q_i e}{4\pi\epsilon_0 m_e}\right)^2\left[\int_0^\infty \frac{\partial f}{\partial v} v^6 dv\right]^{-1} \tag{8}$$

For a Maxwell–Boltzmann distribution, there is an analytical expression:

$$\rho_{\mathrm{MB}} = \left(\frac{-q_i e}{4\pi\epsilon_0}\right)^2 \frac{\sqrt{m_e}}{16e^2}\frac{n_i}{n_e}\ln\Lambda_{ie}\left(\frac{2\pi}{T_e}\right)^{3/2} \tag{9}$$

A similar process gives the Fermi–Dirac equivalent, ρ_{FD}, with $f_{\mathrm{FD}}(v) = f(E)dE/4\pi d^3 v$, though no analytical form of the expression exists as far as we are aware. It is calculated numerically for comparison with the Monte Carlo algorithm.

The resistivity transport coefficient, $\boldsymbol{\alpha}$, is defined by

$$(en_e)^2\mathbf{E} = \boldsymbol{\alpha}\cdot\mathbf{j}$$

In the un-magnetised $\mathbf{B} = \mathbf{0}$ case, only the $\alpha_\parallel = \alpha_\perp(\mathbf{B} = \mathbf{0})$ component of the expansion of $\boldsymbol{\alpha}$ remains, and is often expressed as the dimensionless quantity

$$\alpha_\parallel^c = \alpha_\parallel \frac{\tau}{m_e n_e}$$

where

$$\tau^{-1} = \frac{4\sqrt{2\pi}n_i \ln\Lambda_{ie}}{3\sqrt{m_e}T_e^{3/2}}\left(\frac{q_i e}{4\pi\epsilon_0}\right)^2$$

is the reciprocal of the mean electron–ion collision time.

Fig. 5 shows that a numerically calculated ρ_{FD} based on Eq. (8) is reproduced by the algorithm in the degenerate regime. ρ_{M} is given by Eq. (9) [26]. In both simulation and evaluation of Eq. (8), Pauli blocking of the acceleration by the electric field, and electron–electron collisions are ignored.

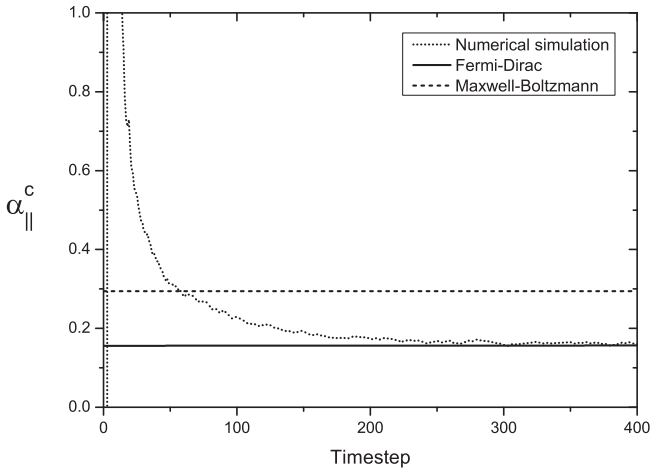

Fig. 5. $\alpha_{\parallel}^{c}$ given by the Monte Carlo algorithm against $\alpha_{\parallel}^{c}$ Maxwell–Boltzmann and Fermi–Dirac distributions according to Eq. (9), with the same T_e. Electron–electron collisions are omitted, $Z = 12$, and there is no blocking of the acceleration by the applied electric field. The initial degeneracy is $\eta = 2.5$.

5. Results

Finally, we present an application of the code in a regime in which other equilibration rates are not applicable. There are situations in inertial confinement fusion in which the validity condition of Eq. (7) is violated, for instance in the interaction between a population of fusion produced alpha particles and a background of cold, dense electrons. It is also inappropriate in this instance because the distribution of fusion produced alpha particles is highly non-Maxwellian. The algorithm as described is capable of modelling both of these features. Fig. 6 shows a situation with parameters approximately similar to inertial confinement fusion; an isotropic flux of monoenergetic fusion produced alpha particles interacting with a cold fuel shell of deuterium, tritium and electrons. At the start of the simulation, $T_\alpha/m_\alpha > T_e/m_e$, and $\eta = 3.2$. The evolution of η is shown in Fig. 8. The trajectory through temperature is different according to the numerical simulation and the degenerate equilibration rate, but the numerical simulation is a more accurate representation of the physics involved in the deposition of energy by alpha particles. For comparison, the numerical simulation is also shown against the non-degenerate equilibration rate in Fig. 7 . The non-degenerate rate predicts a significantly lower T_e throughout the simulation, despite the degeneracy of the numerical simulation being negative for much of the simulation time.

We have presented an algorithm for carrying out calculations on degenerate plasmas using an extension of the well-established binary collision approximation Monte Carlo method. It creates and sustains Fermi–Dirac distributions, gives

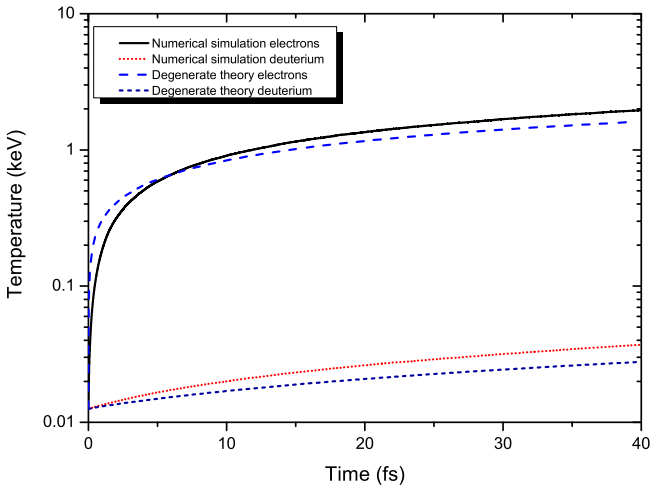

Fig. 6. An equilibration scenario with parameters approximately similar to inertial confinement fusion; starting temperatures of electrons, deuterium and tritium are $T = 12.5$ eV, the density is $n_D = n_T = 1.2 \times 10^{30}\mathrm{m}^{-3}$, $n_\alpha = n_D/10$ and $n_e = 2.6 \times 10^{30}\mathrm{m}^{-3}$. α particles have an initial energy of 3.54 MeV. Only electrons and deuterons are shown. The analytical model is that of the degenerate equilibration rate given by Eq. (7). The evolution of the simulation η over time is shown in Fig. 8.

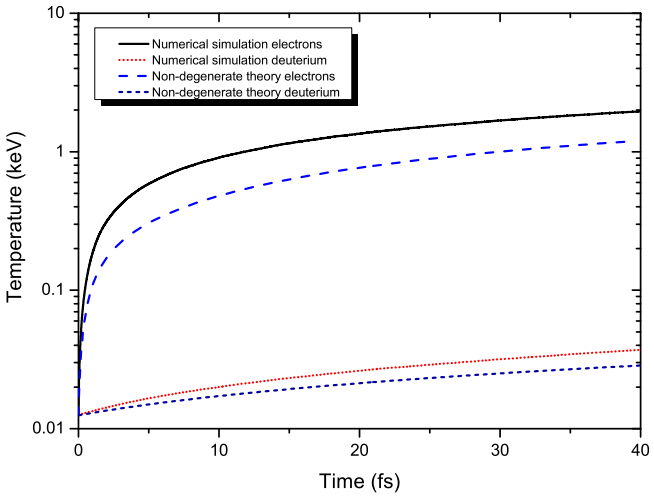

Fig. 7. Numerical simulation of Fig. 6 shown against Spitzer's non-degenerate equilibration rate [24].

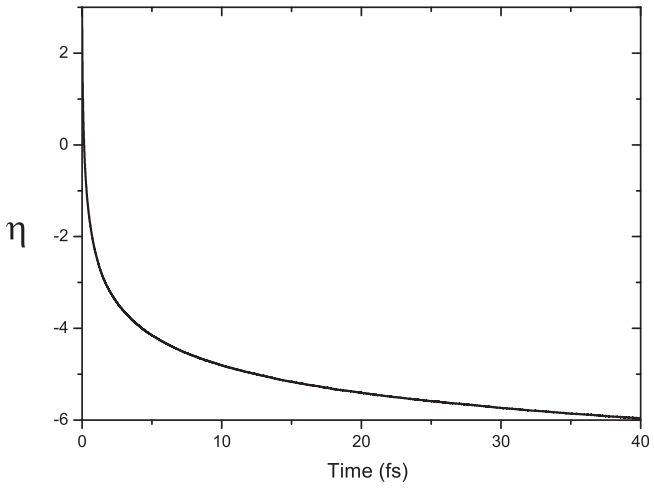

Fig. 8. The degeneracy parameter of the numerical simulation in Figs. 6 and 7 over time from an initial value of $\eta = 3.2$.

degenerate electron–ion equilibration times and stopping powers, and succesfully reproduces the degenerate resistivity transport coefficient for unmagnetised first order transport theory.

We thank the EPSRC for funding this research.

References

[1] T. Takizuka, H. Abe, A binary collision model for plasma simulation with a particle code, Journal of Computational Physics 25 (3) (1977) 205–219, http://dx.doi.org/10.1016/0021-9991(77)90099-7.
[2] A.B. Langdon, Nonlinear inverse bremsstrahlung and heated-electron distributions, Physical Review Letter 44 (1980) 575–579, http://dx.doi.org/10.1103/PhysRevLett.44.575.
[3] R.D. Jones, K. Lee, Kinetic theory, transport, and hydrodynamics of a high-z plasma in the presence of an intense laser field, Physics of Fluids 25 (12) (1982) 2307–2323, http://dx.doi.org/10.1063/1.863712.
[4] R.H. Miller, M.R. Combi, A coulomb collision algorithm for weighted particle simulations, Geophysical Research Letters 21 (16) (1994) 7351738, http://dx.doi.org/10.1029/94GL01835.
[5] K. Nanbu, Theory of cumulative small-angle collisions in plasmas, Physical Review E 55 (1997) 4642–4652, http://dx.doi.org/10.1103/PhysRevE.55.4642.
[6] J. Lindl, Development of the indirect-drive approach to inertial confinement fusion and the target physics basis for ignition and gain, Physics of Plasmas 2 (11) (1995) 3933–4024, http://dx.doi.org/10.1063/1.871025.
[7] Y. Setsuhara, H. Azechi, N. Miyanaga, H. Furukawa, R. Ishizaki, K. Nishihara, M. Katayama, A. Nishiguchi, K. Mima, S. Nakai, Secondary nuclear fusion reactions as evidence of electron degeneracy in highly compressed fusion fuel, Laser and Particle Beams 8 (04) (1990) 609–620, http://dx.doi.org/10.1017/S0263034600009034.
[8] J.P. Cox, R.T. Giuli, Principles of Stellar Structure Volume II: Applications to Stars, Gordon and Breach Science Publishers, 1968.

[9] B. Xu, S.X. Hu, Effects of electron-ion temperature equilibration on inertial confinement fusion implosions, Physical Review E 84 (2011) 016408, http://dx.doi.org/10.1103/PhysRevE.84.016408.
[10] D.O. Gericke, M.S. Murillo, M. Schlanges, Dense plasma temperature equilibration in the binary collision approximation, Physical Review E 65 (2002) 036418, http://dx.doi.org/10.1103/PhysRevE.65.036418.
[11] P. Lugli, D. Ferry, Degeneracy in the ensemble monte carlo method for high-field transport in semiconductors, IEEE Transactions on Electron Devices 32 (11) (1985) 2431–2437, http://dx.doi.org/10.1109/T-ED.1985.22291.
[12] C. Kittel, Introduction to Solid State Physics, John Wiley and Sons, Inc, 2005.
[13] Y.T. Lee, R.M. More, An electron conductivity model for dense plasmas, Physics of Fluids 27 (5) (1984) 1273–1286, http://dx.doi.org/10.1063/1.864744.
[14] L.S. Brown, R.L. Singleton, Temperature equilibration rate with fermi-dirac statistics, Physical Review E 76 (2007) 066404, http://dx.doi.org/10.1103/PhysRevE.76.066404.
[15] S.R. Brown, M.G. Haines, Transport in partially degenerate, magnetized plasmas. Part 2 numerical calculation of transport coefficients, Journal of Plasma Physics 62 (02) (1999) 129–144. <http://dx.doi.org/10.1017/S0022377899007746>.
[16] H. Brysk, P.M. Campbell, P. Hammerling, Thermal conduction in laser fusion, Plasma Physics 17 (6) (1975) 473. <http://stacks.iop.org/0032-1028/17/i=6/a=007>.
[17] E.E. Salpeter, Electrons screening and thermonuclear reactions, Australian Journal of Physics 7 (1954) 373, http://dx.doi.org/10.1071/PH540373.
[18] G.E.P. Box, M.E. Muller, A note on the generation of random normal deviates, The Annals of Mathematical Statistics 29 (2) (1958) 610–611. <http://www.jstor.org/stable/2237361>.
[19] W. Hörmann, J. Leydold, Continuous random variate generation by fast numerical inversion, ACM Transactions on Modelling and Computer Simulation (TOMACS) 13 (4) (2003) 347–362.
[20] C. de Boor, B. Swartz, Piecewise monotone interpolation, Journal of Approximation Theory 21 (4) (1977) 411–416. <http://www.sciencedirect.com/science/article/pii/0021904577900119>.
[21] H.-C. Chen, Y. Asau, On generating random variates from an empirical distribution, AIIE Transactions 6 (2) (1974) 163–166, http://dx.doi.org/10.1080/05695557408974949.
[22] H. Brysk, Electron-ion equilibration in a partially degenerate plasma, Plasma Physics 16 (10) (1974) 927. <http://stacks.iop.org/0032-1028/16/i=10/a=005>.
[23] W.H. Press, S.A. Teukolsky, W.T. Vetterling, B.P. Flannery, Numerical Recipes in C++, Cambridge University Press, 2007.
[24] L. Spitzer, Physics of Fully Ionised Gases, Interscience, New York, 1967.
[25] S.I. Braginskii, Reviews of Plasma Physics, 1, Consultants Bureau, 1965.
[26] E.M. Epperlein, M.G. Haines, Plasma transport coefficients in a magnetic field by direct numerical solution of the Fokker–Planck equation, Physics of Fluids 29 (4) (1986) 1029–1041, http://dx.doi.org/10.1063/1.865901.